Supporting information

For

Interfacial host-guest inclusion complex regulated supramolecular nanocomposite hydrogel showing tunable mechanical strength, self-healing, strain sensitive and NIR responsive

Yuxuan Yang, [a] Yingying Huang, [a] Hongyi Chen, [a] Simin Liu, [a] and Xiongzhi Zhang* [a]

(E-mail: zhangxiongzhi@wust.edu.cn)

[a] School of Chemistry and Chemical Engineering, Institute of Advanced Materials and Nanotechnology,Wuhan University of Science and Technology, Wuhan, 430081, China

Materials

Triethylamine (AR), methylacrylyl chloride (AR), dichloromethane (98%), anhydrous sodium sulfate (98%), concentrated hydrochloric acid, ferric chloride hexahydrate (98%), ethylene glycol (98%), ethanol (98%), sodium acetate (98%) , acetone (98%), adamantan-2-amine hydrochloride (98%), 1-vinylimidazole (98%), benzyl bromide (98%), 4-Vinylbenzyl chloride(90%), Amantadine hydrochloride (99%),1-Adamantylamine (99%), acrylamide (AM, 98%), Boc-1, 6-hexamethylenediamine (98%) and azobis(4-cyanopentanoic acid) (ACVA, 99%) were purchased from Shanghai McLean Biochemical Co., LTD., China. AM was further purified by recrystallization in ethanol. Cucurbit[7]uril (CB[7]) were prepared as our previous work. 1-2 Deionized water was used for all experiments.

Characterization

^{1}H NMR spectra were obtained using Bruker AVIII–600MHz spectrometers. The microstructure of the hydrogels was observed using a scanning electron microscope (SEM, FEI Nova 400 Nano). The sample was freeze-dried for 48 hours coated with a thin layer of gold before SEM images were taken.

Rheological tests were carried out on a TA DHR-2 equipped with a temperature controller. The storage modulus (G') and loss modulus (G'') were measured in three rheological experiments. The tests were performed on 20 mm diameter parallel–plate geometry in a gap size of 1 mm. The three experiments conducted are the following: (i) Oscillatory strain sweeps (1-100%), in order to obtain the linear viscoelastic region for the time sweeps, were conducted at 25 ºC with a fixed frequency of 1Hz; ii) Dynamic oscillatory frequency sweep measurements were conducted at a 5% strain amplitude, between 0.1 and 10 Hz; iii) Time scan tests were performed with an alternating strain of 5% and 200%, with a fixed frequency (1 Hz) at 25 ºC.

Tensile tests were performed, on a tensile tester (SUNS Technology) equipped with a 5-N load cell, at a deformation rate (50 mm min^{-1}). In order to avoid systematic failure in the vicinity of the clamps, all the samples were cut using a dumbbell-shaped die cutter following the ISO4661-1 standard with the reduced section of the samples. In the compression test, samples with cylinder shapes were placed on a metal plate coated with silicon oil to decrease friction, at a loading velocity of 1 mm min^{-1}.

The hydrogel was cut into two parts and two surfaces were brought together to heal. The healing

efficiency of strain (*f*) was determined by $f_1 = \varepsilon/\varepsilon_0$, where ε and ε_0 are the breaking strain of the healed sample and the original sample, respectively. The healing efficiency determined by stress is $f_2 = \delta/\delta_0$, where δ and δ_0 are the breaking stress of the healed sample and the original sample, respectively. The fracture toughness was characterized by the fracture energy (U, MJ m^3), which was calculated by integrating the area under the stress–strain curve:

$$U = \int \sigma d\varepsilon$$

The NIR photothermal response of the as-obtained hydrogel was carried out by NIR laser light (808 nm, Changchun New Industries Optoelectronics). The hydrogels with the same volume were exposed to NIR laser light at a distance of 3 cm. The heat maps of hydrogels were recorded at a specific time by an infrared camera.

The strain-dependent resistance changes of the hydrogel were demonstrated by the stretched or compressed hydrogel. After that, the hydrogel acts as a wearable flexible strain sensor, adhering to the different surfaces of the human body, connecting with an electrochemical workstation (PGSTAT302N, Metrohm) via metal wires with a fixed voltage of 1.5 V. The signals of the resistance changes were recorded on the electrochemical workstation to monitor the various movements of the human body. The relative resistance variation was calculated based on the equation: $\Delta R/R_0 = (R - R_0)/R_0 \times 100\%$, where R_0 and R represent the original resistance and resistance at different strains, respectively.

The cytotoxicity of P(AM-G_1)-Fe_3O_4@CB[7] hydrogels with different contents was evaluated by MTT assay. The Dulbecco's modified Eagle's medium (DMEM) supplemented with 10% fetal bovine serum (FBS; heat inactivated) and 1% antibiotic-antimycotic solution (1000 U/mL penicillin G, 10 mg/mL streptomycin sulphate, 5 mg/mL gentamcin, and 25 μg/mL amphotericin B) was used to maintain the 3T3 fibroblast cells. The cells were seeded in a 96-well plate with DMEM containing serum and maintained at 37 °C in a humidified incubator (Heal Force, HF 160W, China) supplemented with 5% CO_2. The extraction media obtained after 24 h were added to the wells containing 3T3 fibroblast cells and incubated for 24 h. The media was removed after 24 h of treatment and cells were washed with phosphate-buffered saline (PBS; 0.01 mol L^{-1}, pH = 7.2) followed by the addition of 100 μL of MTT (0.5 mg/mL) prepared in serum free medium to each well and incubated for 6 h.

Experimental Section

Synthesis of Fe_3O_4@CB[7] MNPs

$FeCl_3$•$6H_2O$ and CB[7] were dispersed in glycol (20 mL), sodium acetate (1.2 g) was added and stirred for 30 min, transferred to a hot kettle for reaction at 200 °C for 10 h, then cooled to room temperature and the black powders were washed three times with deionized water and ethanol.

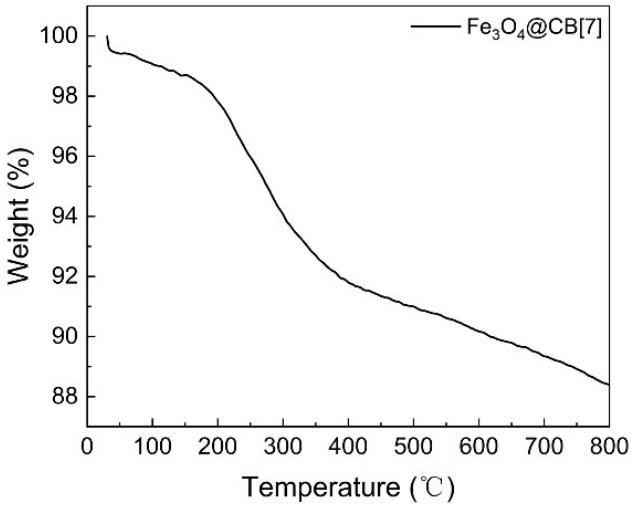

Fig. S1 TGA curves of Fe_3O_4@CB[7] MNPs.

Synthesis of N, N-dimethyladamantaneamine

18.7 g (0.1mol) of amantadine hydrochloride, 20mL of water, 21mL of 88% formic acid, and 34 mL of 40% formaldehyde were added to the round-bottom flask. The mixture was refluxed at 60 °C for 15 hours. Subsequently, neutralize the reaction solution with a saturated solution of NaOH and adjust the pH to 11-12. The solution was extracted with dichloromethane. Dry the extract with anhydrous sodium sulfate and rotate to evaporate the dichloromethane, a colorless solid was obtained.

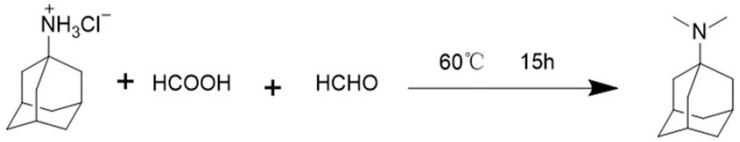

Fig. S2 Synthesis process of N, N-dimethyladamantaneamine.

Synthesis of G_1

8.7 g of N, N-dimethyladamantaneamine (0.05 mol) and 9.2 g of p-chloromethylstyrene (0.06 mol) were added to the round-bottom flask and dissolved in 50 mL of methanol. The reaction was conducted for 12 hours at 50 °C. The solvent was added to ether, and white precipitate was produced. The white precipitate was washed three times with ether to obtain the product. ^{1}H NMR (600 MHz, D_2O) δ (ppm): 7.64 (d, J = 7.9 Hz, 1H), 7.53 (d, J = 8.0 Hz, 1H), 6.91 – 6.83 (m, 1H), 5.97 (d, J = 17.7 Hz, 1H), 5.44 (dd, J = 11.0, 3.6 Hz, 1H), 4.42 (d, J = 3.8 Hz, 2H), 2.80 (s, 2H), 2.40 (s, 3H), 2.26 (d, J = 3.8 Hz, 6H), 1.83 – 1.71 (m, 6H).

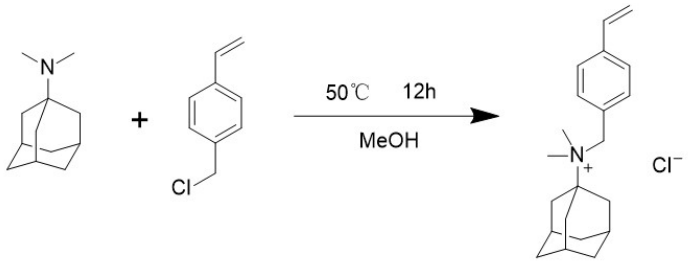

Fig. S3 Synthesis process of G_1.

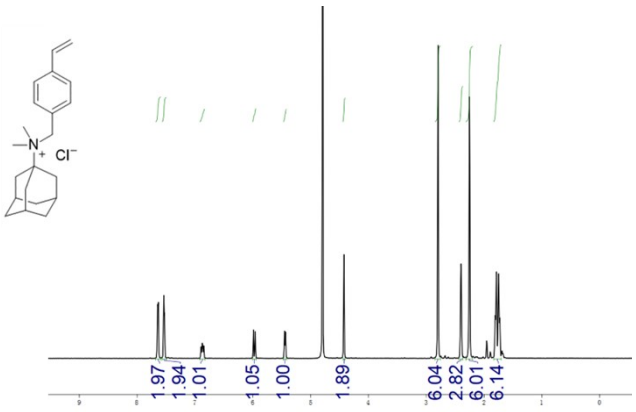

Fig. S4 ^{1}H NMR spectrum (600 MHz, D_2O) of G_1.

Synthesis of G_2

Amantadine and triethylamine (0.7 g, 6.92 mmol) were added to a 50 mL round-bottom flask, and 20 mL of anhydrous dichloromethane was added. Methacryloyl chloride (0.29 g, 2.76 mmol) was dissolved in 10 mL of anhydrous dichloromethane. The solution of methyl acrylyl chloride was slowly added within an ice water bath, reacted at room temperature for 10 h, and then extracted three times with an aqueous solution of $NaHCO_3$. The organic phase was removed by rotary evaporation to obtain the product. ^{1}H NMR (600 MHz, $CDCl_3$) δ (ppm): 5.56 (s, 1H), 5.44 (s, 1H), 5.23 (t, J = 1.5 Hz, 1H), 2.12–2.05 (m, 3H), 2.02 (d, J = 2.9 Hz, 6H), 1.91 (d, J = 1.3 Hz, 3H), 1.70 – 1.64 (m, 7H).

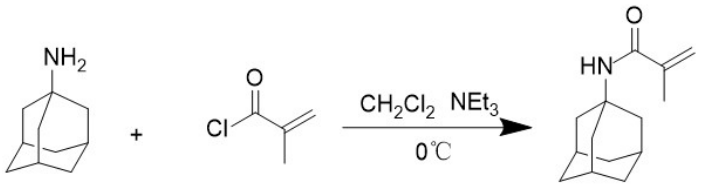

Fig. S5 Synthesis process of G_2.

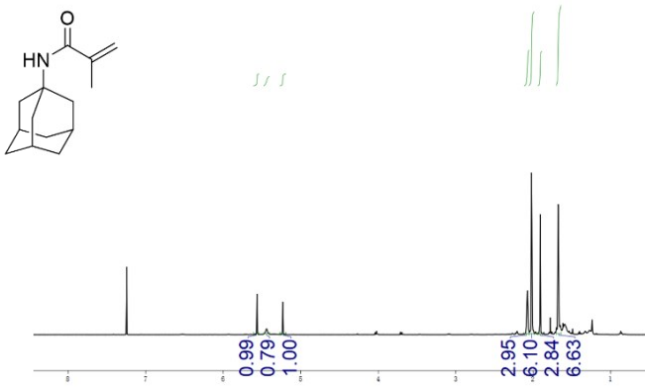

Fig. S6 ^{1}H NMR spectrum (600 MHz, $CDCl_3$) of G_2.

Synthesis of G_3

N, N-dimethylferrocenylamine (2.0 g, 8.23 mmol) was added to a 50 mL round-bottomed flask and 10 mL of ether solvent was added. p-chloromethyl styrene (1.88 g, 12.34 mmol) was dissolved in 10 mL of ether. The solution of p-chloromethyl styrene was slowly added within an ice water bath and reacted at room temperature for 24 h. A yellow solid was formed at the bottom of the flask. The yellow solid was washed three times with ether to remove the white precipitate. ^{1}H NMR (600 MHz, $CDCl_3$) δ

(ppm): 7.62 (s, 2H), 7.46 (s, 2H), 6.71 (dd, *J* = 17.2, 10.5 Hz, 1H), 5.82 (d, *J* = 17.0 Hz, 1H), 5.36 (d, *J* = 10.2 Hz, 1H), 4.94 (s, 4H), 4.53 (s, 2H), 4.35 (s, 2H), 4.29 (s, 4H), 3.04 (s, 6H).

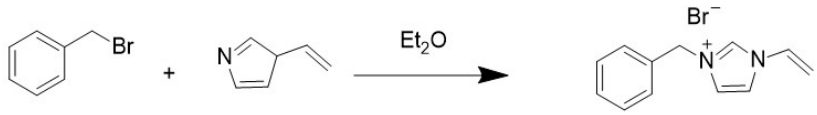

Fig. S7 Synthesis process of G_3.

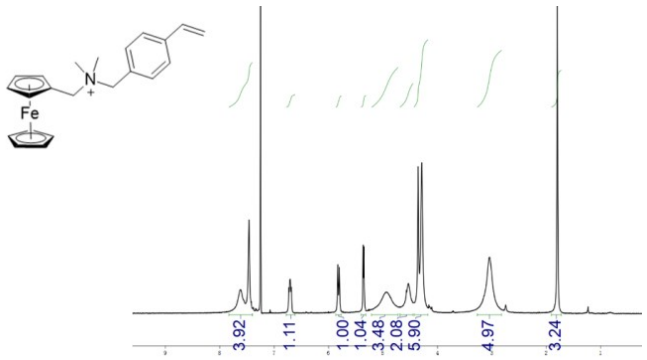

Fig. S8 ^{1}H NMR spectrum (600 MHz, $CDCl_3$) of G_3.

Synthesis of G_4

5 g of benzyl bromide was dissolved in 20 mL of ethyl ether and added to a (2.75 g) solution of 1-vinylimidazole in ether (10 mL) under the condition of an ice bath. The reaction continued at room temperature for 12 h. As the reaction progressed, a white precipitate was formed. After the reaction, the white precipitate was filtered, washed with ether three times, and finally dried under vacuum. ^{1}H NMR (600 MHz, D_2O) δ (ppm): 8.90 (s, 1H), 7.64 (d, J = 2.3 Hz, 1H), 7.43 (s, 1H), 7.36 (dd, J = 5.1, 1.9 Hz, 3H), 7.31 (dd, J = 7.0, 2.8 Hz, 2H), 6.98 (dd, J = 15.6, 8.7 Hz, 1H), 5.65 (dd, J = 15.6, 2.8 Hz, 1H), 5.29 (d, J = 12.5 Hz, 3H).

Fig. S9 Synthesis process of G_4.

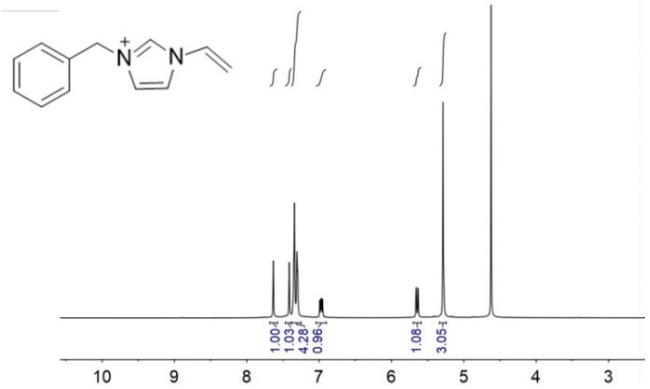

Fig. S10 ^{1}H NMR spectrum (600 MHz, D_2O) of G_4.

Synthesis of the monomer N-Boc-N'-methacrylamide-1, 6-diaminohexane

The compounds N-tert-butoxycarbonyl-1, 6-hexanediamine (0.5 g, 2.31 mmol), triethylamine (0.7 g,

6.92 mmol) were dissolved in 20 mL of anhydrous dichloromethane. A solution of methacryloyl chloride (0.29 g, 2.76 mmol) was slowly added within an ice bath. The reaction mixture was maintained at room temperature for 12 h. The reaction mixture was concentrated, washed with water, $NaHCO_3$ solution, and NaCl solution. The organic layer was collected and the solvent was removed with a rotary evaporator. [3]

Synthesis of G_5

N-Boc-N′-methacrylamide-1, 6-diaminohexane (0.3 g) was dissolved in methanol (20 mL), hydrochloric acid (12 mol/L, 5 mL) was added, and the solution was stirred at room temperature for 5 h. The solution was precipitated in ether to obtain the product. [4] ^{1}H NMR (600 MHz, DMSO-d_6) δ (ppm): 8.07 – 7.82 (m, 6H), 5.62 (s, 1H), 5.29 (s, 1H), 3.16 – 2.98 (m, 3H), 2.74 (h, J = 6.1 Hz, 2H), 1.84 (s, 2H), 1.53 (h, J = 6.8, 6.4 Hz, 2H), 1.42 (t, J = 14.6, 7.4 Hz, 2H), 1.35 – 1.17 (m, 5H).

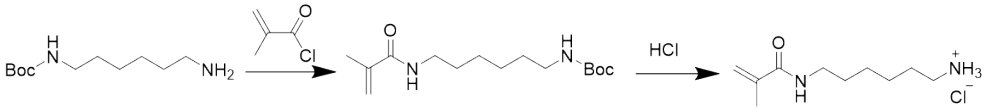

Fig. S11 Synthesis process of G_5.

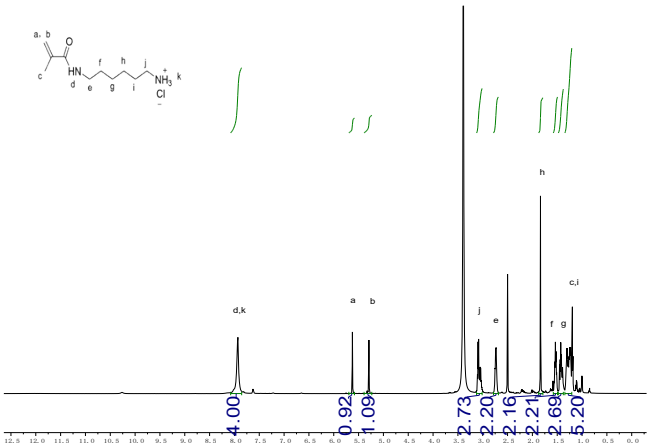

Fig. S12 ^{1}H NMR spectrum (600 MHz, DMSO-d_6) of G_5.

Synthesis of P(AM-G_1)-Fe_3O_4@CB[7]$_X$

Acrylamide (1 g), 0.23 g of guest G_1, and 30 mg of ACVA were dissolved in 20 mL of H_2O, and the reaction was carried out within a nitrogen atmosphere for 24 h at 60 °C. The product was precipitated with acetone, and then washed with acetone for three times, vacuum-dried to obtain P(AM-G_1) polymer chain. Fe_3O_4@CB[7] MNPs with different contents were added to the P (AM-G_1) solution to obtain P (AM-G_1)-Fe_3O_4@CB[7]$_X$. It is estimated that the grafting ratio of G_1 to AM is about 1 : 5 by the integral ratio of proton hydrogen on the ring to H_{14}, H_{17}, H_{15} and H_{16} in ^{1}H NMR.

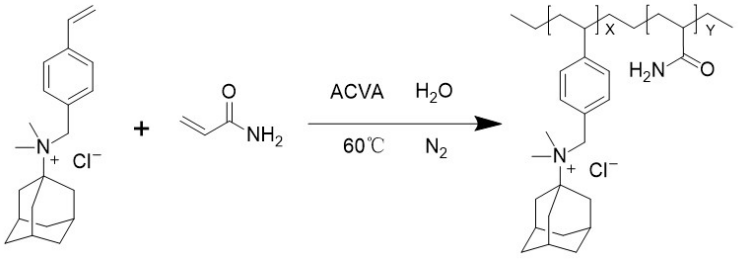

Fig. S13 Synthesis process of P(AM-G_1).

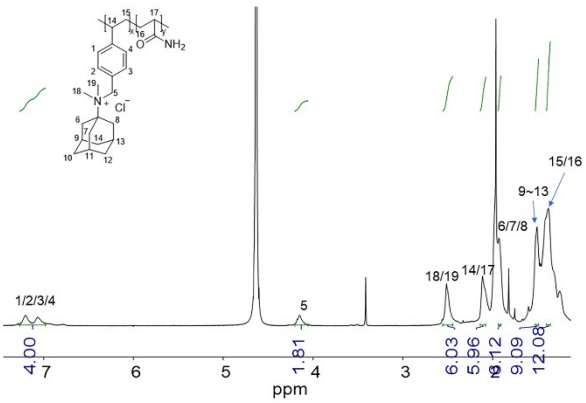

Fig. S14 ^{1}H NMR spectrum (600 MHz, D_2O) of P(AM-G_1).

Synthesis of P(AM-G_2)-Fe_3O_4@CB[7]$_X$

Acrylamide (1 g), G_2 (0.15 g), and AIBN (30 mg) were dissolved in 20 mL of DMSO and the reaction mixture was degassed using three freeze-pump-thawing cycles. The polymerization system was placed in an oil bath at 60 °C for 10 h. After polymerization, the polymer solution was added to the diethyl ether (30 mL) to obtain a white precipitate. Fe_3O_4@CB[7] MNPs were added to the P (AM-G_2) solution to obtain P (AM-G_2) Fe_3O_4@CB[7]$_X$. According to the integral ratio of H_1 to H_2 in ^{1}H NMR, the estimated grafting ratio of G_2 to AM is about 1 : 4.

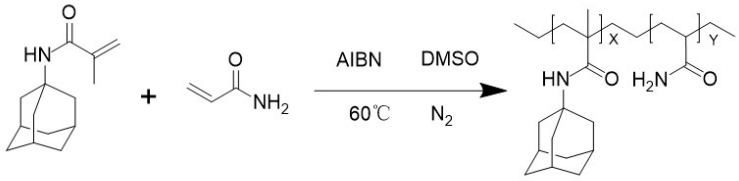

Fig. S15 Synthesis process of P(AM-G_2).

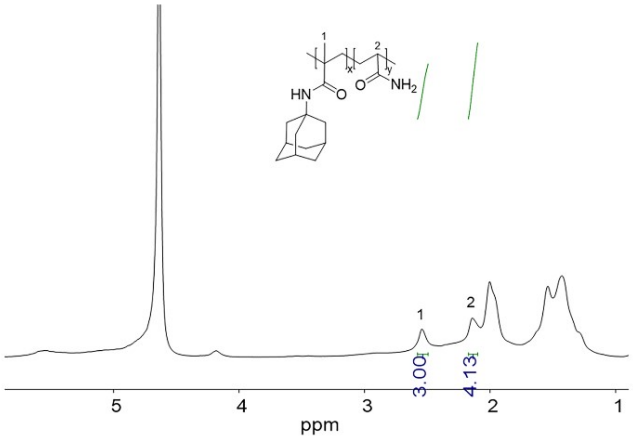

Fig. S16 ^{1}H NMR spectrum (600 MHz, D_2O) of P(AM-G_2).

Synthesis of P(AM-G_3)-Fe_3O_4@CB[7]$_X$

Acrylamide (1 g), G_3 (0.287 g), and AIBN (30 mg) were dissolved in 20 mL of DMSO and the reaction mixture was degassed using three freeze-pump-thawing cycles. The polymerization system was placed in an oil bath at 60°C for 10 h. After polymerization, the polymer solution was added to the diethyl ether (30 mL) to obtain a white precipitate. Fe_3O_4@CB[7] MNPs were added to the P (AM-G_3) solution to obtain P (AM-G_3)-Fe_3O_4@CB[7]$_X$. According to the integral ratio of H_6 and H_7 in ^{1}H NMR,

the estimated grafting ratio of G_3 to AM is about 1 : 3.

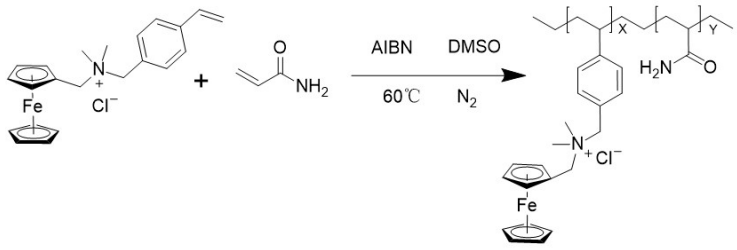

Fig. S17 Synthesis process of P(AM-G_3).

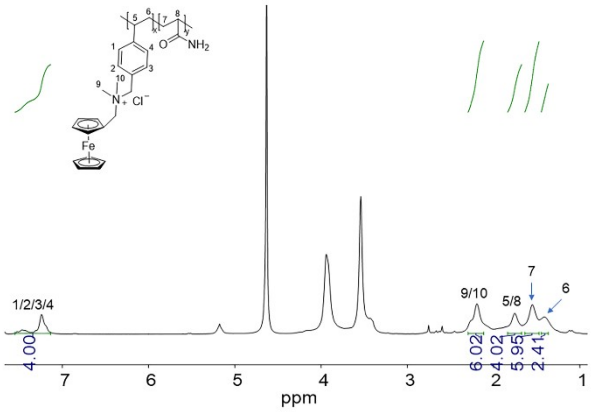

Fig. S18 ^{1}H NMR spectrum (600 MHz, D_2O) of P(AM-G_3).

Synthesis of P(AM-G_4)-Fe_3O_4@CB[7]$_X$

Acrylamide (1 g), G_4 (0.185 g), and ACVA (30 mg) were dissolved in 20 mL of water and the reaction mixture was degassed using three freeze-pump-thawing cycles. The polymerization system was carried out at 60 °C for 8 h. After polymerization, the polymer solution was added to the diethyl ether (30 mL) to obtain a white precipitate. Fe_3O_4@CB[7] MNPs were added to the P (AM-G_4) solution to obtain P (AM-G_4)-Fe_3O_4@CB[7]$_X$. According to the integral ratio of H_8 to H_{11} in ^{1}H NMR, the grafting ratio of G_4 to AM was estimated to be 1 : 6. According to the integral ratio of H_1 to H_2 in ^{1}H NMR, the estimated grafting ratio of G_4 to AM is about 1 : 4.

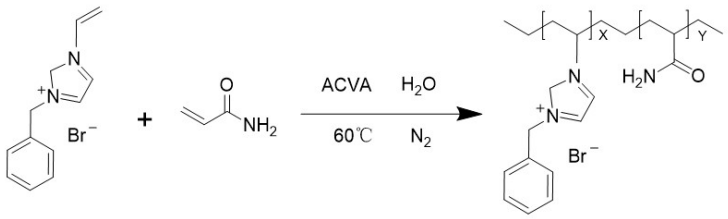

Fig. S19 Synthesis process of P(AM-G_4).

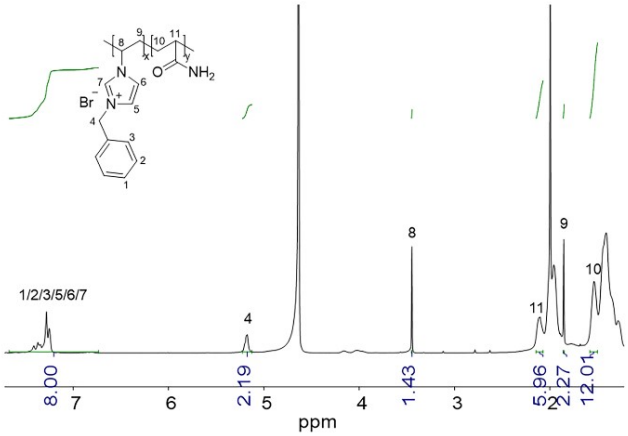

Fig. S20 ^{1}H NMR spectrum (600 MHz, D_2O) of P(AM-G_4).

Synthesis of P(AM-G_5)-Fe_3O_4@CB[7]$_X$

The acrylamide (1 g), G_5 (0.15 g), and ACVA (30 mg) were dissolved in 20 mL of water and the reaction mixture was degassed using three freeze-pump-thawing cycles. The polymerization system was placed in an oil bath at 60 °C for 5 h. After polymerization, the polymer solution was added to the diethyl ether (30 mL) to obtain a white precipitate. Fe_3O_4@CB[7] MNPs were added to the P (AM-G_5) solution to obtain P (AM-G_5)-Fe_3O_4@CB[7]$_X$. According to the integral ratios of H_1 and H_6 to H_7 and H_{10} in ^{1}H NMR, the estimated grafting ratio of G_5 to AM is about 1 : 5.

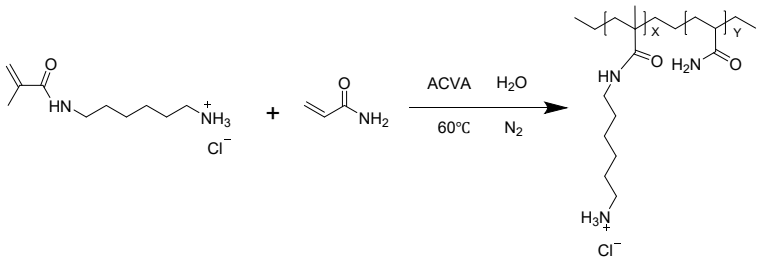

Fig. S21 Synthesis process of P(AM-G_5).

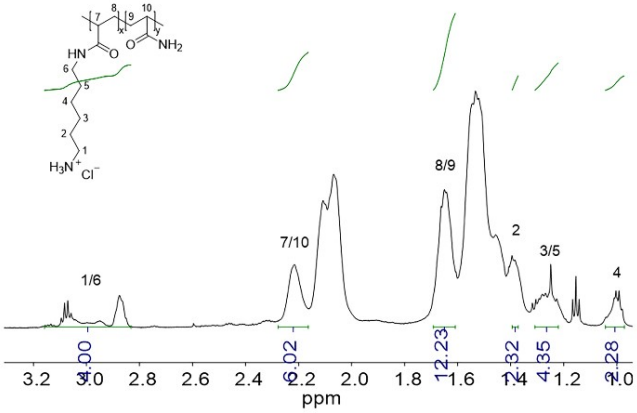

Fig. 22 ^{1}H NMR spectrum (600 MHz, D_2O) of P(AM-G_5).

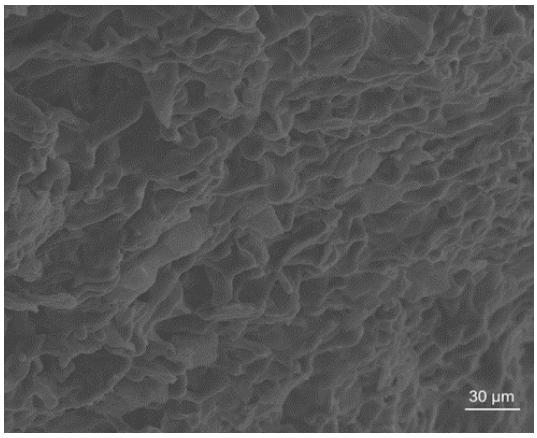

Fig. S23 SEM of the P(AM-G_1) polymer.

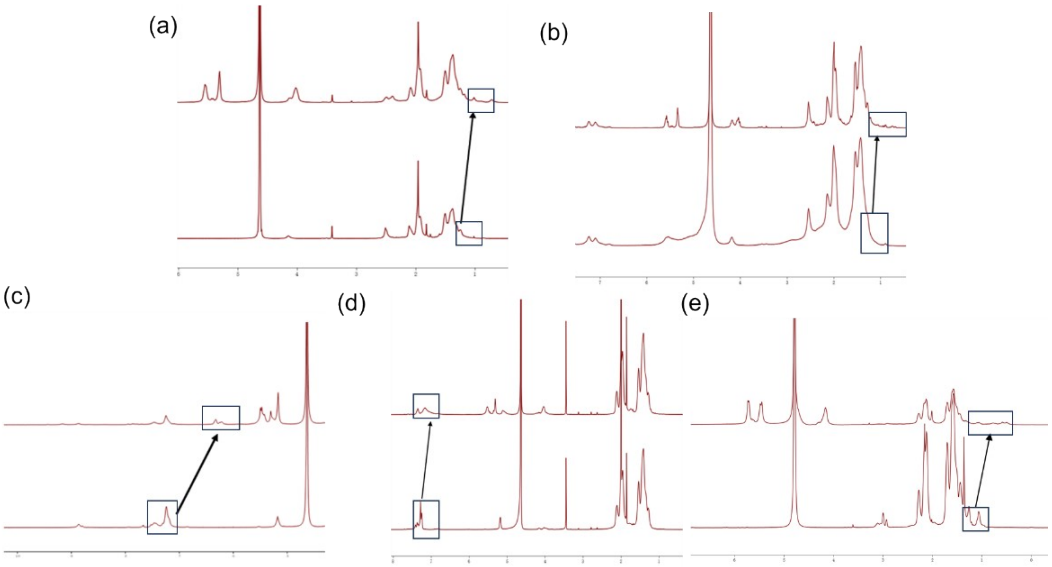

Fig. S24 ^{1}H NMR spectra (600 MHz, D_2O) of P(AM-G) and P(AM-G) after the addition of CB[7], the gusts rang from G_1-G_5.

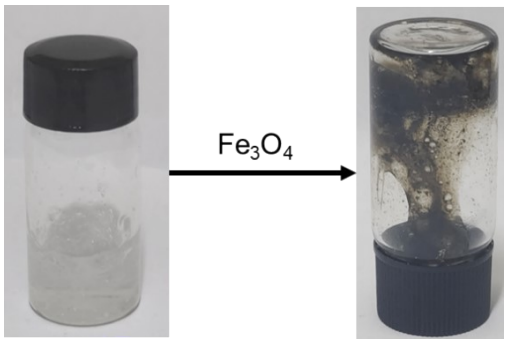

Figure S25. Pictures of P(AM-G_1) solution added with Fe_3O_4.

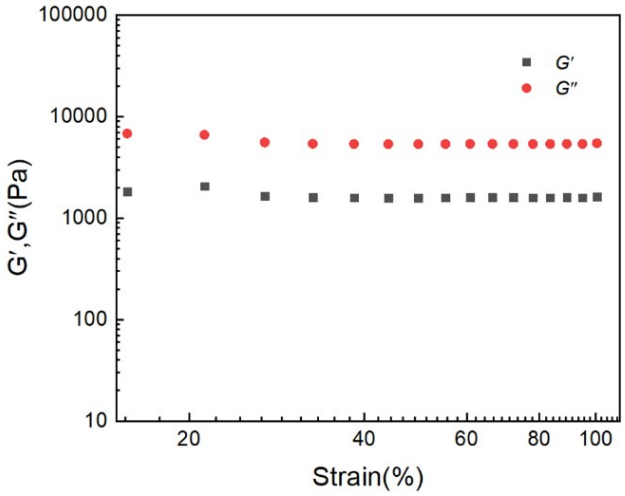

Fig. S26 Strain sweep rheological of P(AM-G_1) solution added with Fe_3O_4.

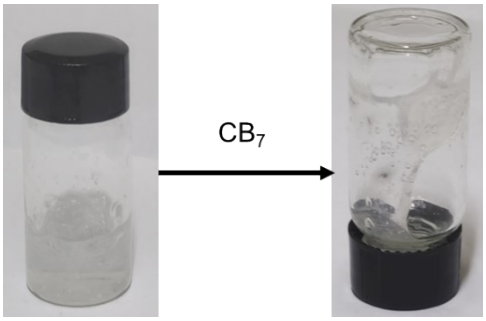

Fig. S27 Pictures of P(AM-G_1) solution added with CB [7].

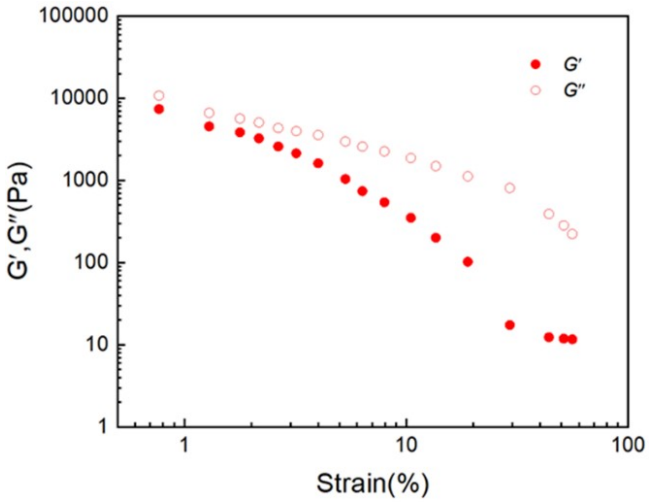

Fig. S28 Strain sweep rheological of P(AM-G_1) solution added with CB[7].

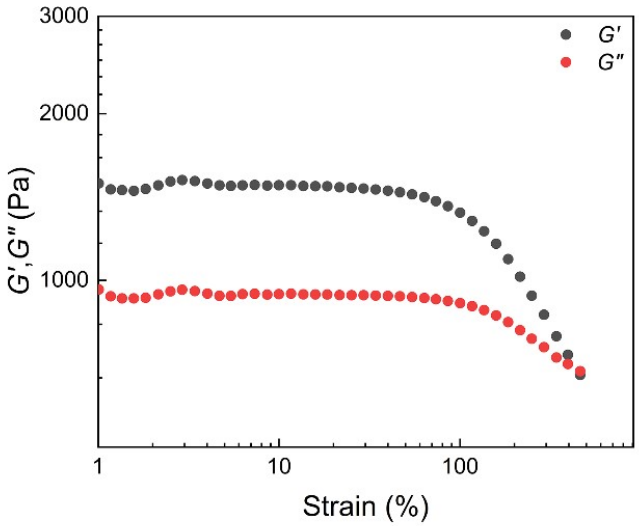

Fig. S29 Strain sweep of P(AM-G_2)·Fe_3O_4@CB[7]$_7$.

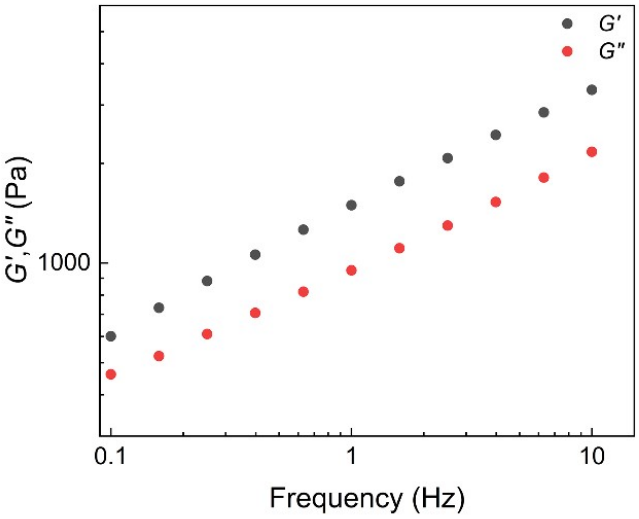

Fig. S29 Frequency sweep of P(AM-G_2)·Fe_3O_4@CB[7]$_7$.

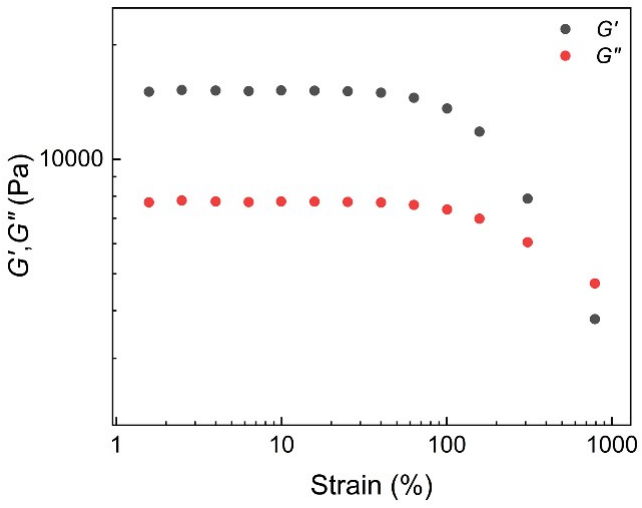

Fig. S30 Strain sweep of P(AM-G_3)·Fe_3O_4@CB[7]$_7$.

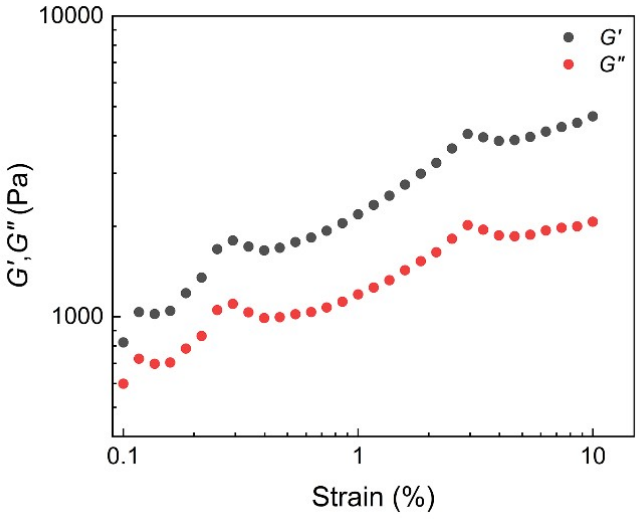

Fig. S31 Frequency sweep of P(AM-G_3)·Fe_3O_4@CB[7]$_7$.

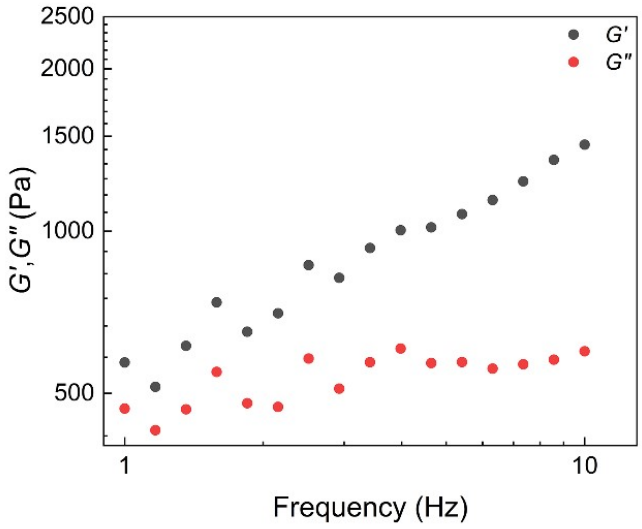

Fig. S32 Strain sweep of P(AM-G_4)·Fe_3O_4@CB[7]$_7$.

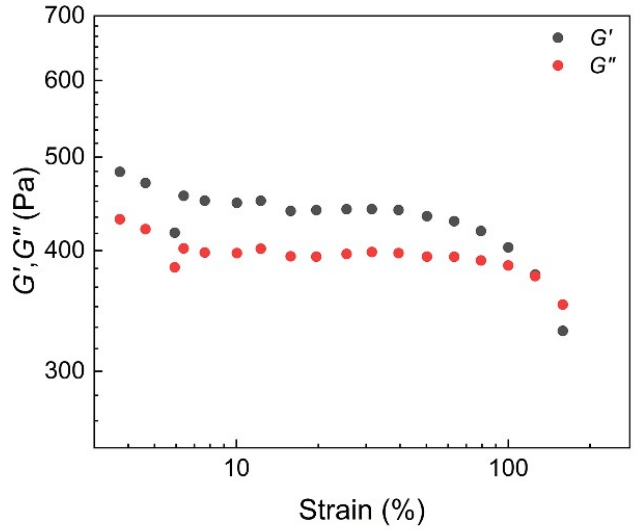

Fig. S33 Frequency sweep of P(AM-G_4)·Fe_3O_4@CB[7]$_7$.

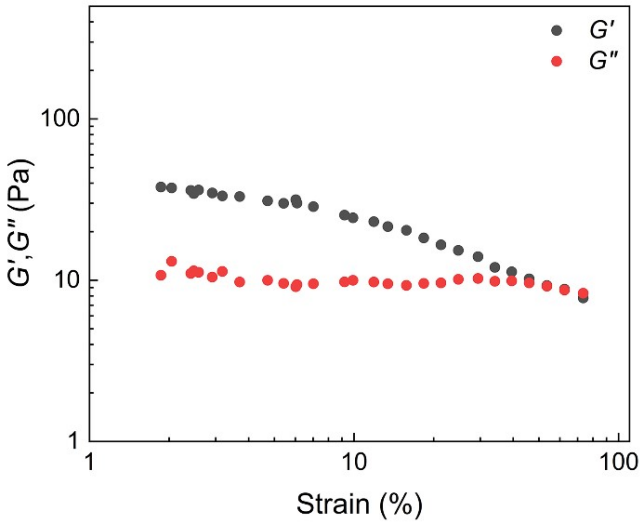

Fig. S34 Strain sweep of P(AM-G_5)·Fe_3O_4@CB[7]$_7$.

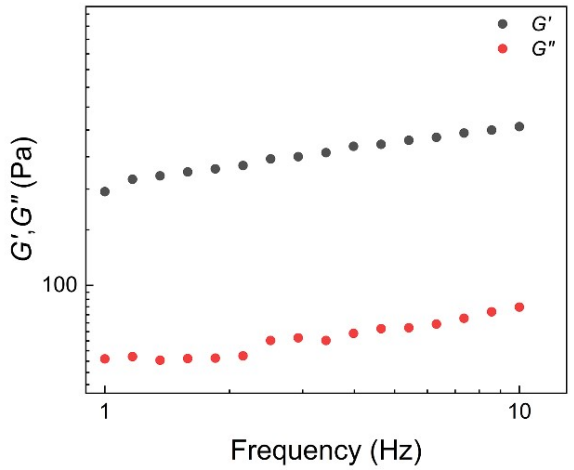

Fig. S35 Frequency sweep of P(AM-G_5)·Fe_3O_4@CB[7]$_7$.

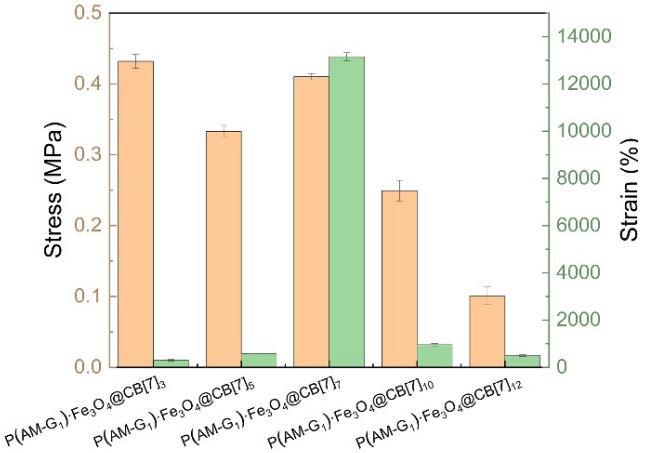

Fig. S36 Tensile stress−strain curves of hydrogel with different Fe_3O_4@CB[7] contents.

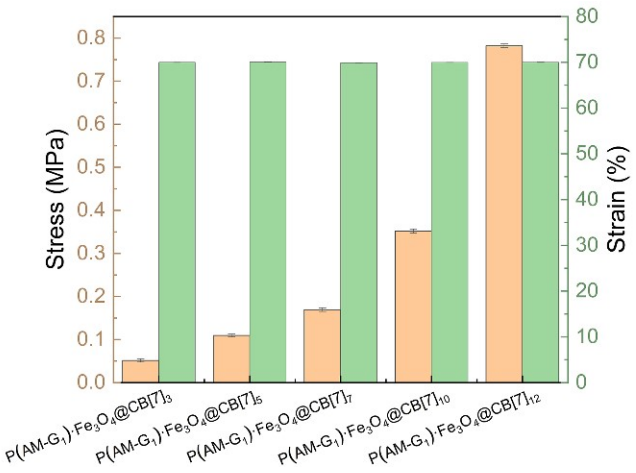

Fig. S37 Compression curves of hydrogel with different Fe_3O_4@CB[7] contents

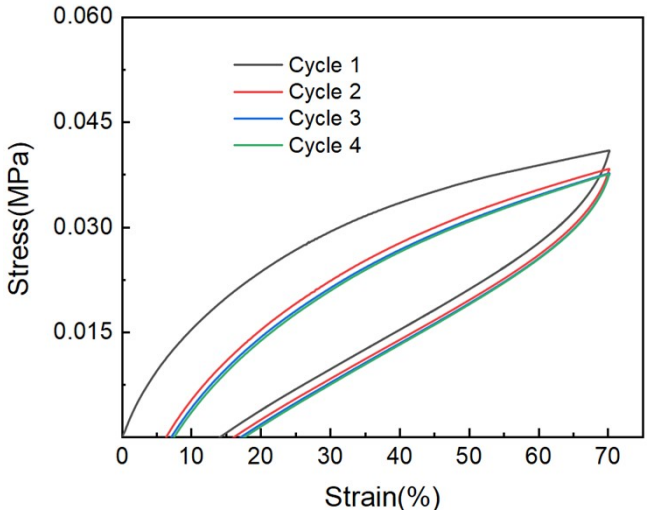

Fig. S38 Tensile curves of loading–unloading cycles of P(AM-G)·Fe_3O_4@CB[7]$_7$ hydrogel.

CB[7] guest	log k	method
	14.32	ITC
	12.60	ITC
	12.62	NMR
	6.35	ITC
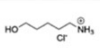	4.30	NMR

Fig. S39 Association constants reported for CB[7]inclusion complexes with different gusts.[5]

References

1. Day, A.; Arnold, A. P.; Blanch, R. J.; Snushall, B., *The Journal of Organic Chemistry* **2001,** *66* (24), 8094-8100.

2. Winter, H. H.; Chambon, F., *J. Rheol.* **1986,** *30* (2), 367-382.

3. Sahl, M.; Muth, S.; Branscheid, R.; Fischer, K.; Schmidt, M., *Macromolecules* **2012,** *45* (12), 5167-5175.

4. Houghten, R. A.; Beckman, A.; Ostresh, J. M., *Int. J. Pept. Protein Res.* **2009,** *27* (6), 653-658.
5. Barrow, S. J.; Kasera, S.; Rowland, M. J.; del Barrio, J.; Scherman, O. A., *Chem. Rev.* **2015,** *115* (22), 12320-12406.